Equivalent: Jurnal Ilmiah Sosial Teknik
Volume 8, Issue 5, 1927-1940
e_ISSN: 2775-0833
https://jurnalequivalent.id/index.php/jequi/index
DOI: doi.org/10.59261/jequi.v8i5.462

Geometric Optimization of Mine Haul Roads Based on Cycle Time and Rolling Resistance Analysis to Improve Haul Truck Productivity

Achmad Pahrul Rodji* Universitas Krisnadwipayana, Indonesia
Indriasari Universitas Krisnadwipayana, Indonesia
Rifki Hilmansyah Universitas Krisnadwipayana, Indonesia

***Corresponding author:**
Achmad Pahrul Rodji, Universitas Krisnadwipayana, Indonesia.
✉ achmadpahrulrodji@unkris.ac.id

Article Info:
Article history:
Received: September 09, 2026
Revised: October 09, 2026
Accepted: October 12, 2026
Available Online: October 23, 2026

***Keywords*:**
Cycle Time;
Haul Truck Productivity;
Mine Haul Road;
Road Geometry;
Rolling Resistance;

This is an open access article under the CC BY-SA license.

Copyright © 2026 by Author. Published by Politeknik Siber Cerdika International

Abstract

Background: Mine haul road conditions directly influence haul truck speed, cycle time, and operational productivity. At Sector 7 of PT Asmin Bara Bronang, overburden haulage had not met the production target, and several road segments did not satisfy the geometric design criteria specified in Ministerial Decree No. 1827 K/30/MEM/2018.
Objective: This study evaluates the existing haul road geometry and estimates the potential productivity improvement achievable by redesigning deficient road segments.
Methods: A quantitative descriptive-evaluative approach was applied to 38 road segments along a 3,038 m haul route. Field measurements covered road width, grade, superelevation, crossfall, rolling resistance, and the cycle time of the Komatsu HD785-7 haul truck. Haul truck performance under idealized geometric conditions was simulated using TALPAC.
Results: The required improvements included increasing the average width by 4.56 m on deficient straight segments and by 5.10 m on deficient curved segments, reducing the average grade by 1.5%, increasing the average superelevation by 2.7%, establishing a 2% crossfall, and reducing rolling resistance to 2.45%. Productivity increased from 92.627 to 124.564 bcm/h.
Conclusion: Bringing haul road geometry into compliance with the applicable design criteria can substantially improve haulage efficiency, with an estimated productivity gain of 31.94 bcm/h.

To cite this article: Rodji, A. P., Indriasari, & Hilmansyah, R. (2026). Geometric optimization of mine haul roads based on cycle time and rolling resistance analysis to improve haul truck productivity. *Equivalent: Jurnal Ilmiah Sosial Teknik*, *8*(5), 1927-1940. https://doi.org/10.59261/jequi.v8i5.462

INTRODUCTION

Open-pit coal mining is characterized by a sequence of highly interconnected operations, including land clearing, overburden removal, coal extraction, material handling, processing, and transportation to disposal areas, stockpiles, or port facilities. Among these activities, material haulage represents one of the most operationally intensive components because it relies on the continuous interaction of heavy equipment, road infrastructure, material characteristics, and production scheduling (Kodikara et al., 2024; Saputra et al., 2023; X. Yang et al., 2024). The effectiveness of the haulage system therefore directly influences the continuity and reliability of mine production. At PT Asmin Bara Bronang in Central Kalimantan, overburden transportation from the mining face to the Sector 7 disposal area constitutes a critical operational process because delays or inefficiencies along the haul route may constrain the achievement of planned production targets.

The increasing scale of contemporary open-pit mining has intensified the need for haulage systems that can transport large volumes of material while maintaining operational efficiency

under variable field conditions. Modern mining operations increasingly emphasize productivity improvement, equipment utilization, cost efficiency, operational reliability, and data-driven engineering decision-making. Within this context, haul-road infrastructure should not be regarded merely as a supporting facility but as an integral component of the production system. Mechanical haulage productivity is principally influenced by payload, cycle time, effective working time, equipment performance, and road conditions encountered during operation (Alshboul et al., 2026; Feng et al., 2025; Jerden et al., 2024). Consequently, inadequate or deteriorating road geometry can generate cumulative operational losses even when the hauling equipment itself possesses sufficient nominal capacity.

Haul-road geometry strongly influences the ability of haul trucks to operate at appropriate and stable speeds. Insufficient carriageway width may restrict vehicle maneuverability and safe passing, particularly on two-way roads, while excessive longitudinal grades increase traction requirements during loaded travel and braking demands during downhill travel. Similarly, inadequate superelevation on curves can adversely affect vehicle stability, whereas insufficient crossfall can reduce surface drainage efficiency and accelerate the formation of ruts, depressions, and potholes. These surface defects subsequently increase rolling resistance and require haul trucks to generate additional tractive effort (Basharaf et al., 2026; Jafarsalehi et al., 2025; Mousavi et al., 2025). The combined effects may reduce average travel speed, extend haulage cycle time, increase fuel consumption and equipment demands, and ultimately reduce hourly production capacity.

This issue also has broader engineering and operational significance. Haul-road deficiencies can affect not only productivity but also operational reliability, road-maintenance requirements, equipment wear, fuel consumption, and the working conditions of haul-truck operators. From an engineering management perspective, maintaining appropriate road geometry is therefore essential to balancing production objectives with safe and sustainable operations. In Indonesia, these considerations are reinforced by the technical requirements established in Ministerial Decree No. 1827 K/30/MEM/2018, which provides guidelines for good mining engineering practices. Compliance with these requirements provides an important technical basis for the design and maintenance of haul roads used by large mining equipment.

Recent academic developments have increasingly incorporated digital technologies, simulation, computer vision, automation, and optimization into the evaluation of open-pit mining transportation systems. Studies have addressed mine-road monitoring using unmanned aerial vehicles and deep-learning approaches, autonomous mining vehicles, intelligent road extraction, and mine-road network optimization (Saputra et al., 2023; Y. Yang et al., 2024; Zhao et al., 2025). These developments demonstrate a broader transition toward data-driven and digitally supported mine-haulage management. However, sophisticated operational technologies remain dependent on suitable physical road conditions. Consequently, optimizing fundamental road parameters, such as width, grade, superelevation, crossfall, and rolling resistance, remains highly relevant even as mining operations progress toward automation and intelligent transportation systems.

Previous studies have examined the relationships among road conditions, transportation systems, equipment operation, and productivity. Nevertheless, many investigations have focused on individual geometric parameters, road-condition assessments, or cycle-time modeling separately rather than integrating segment-level road geometry and rolling-resistance variations within a unified operational assessment framework (Ascaso Til & Wong, 2023; Görçün et al., 2024; Soto-Diaz et al., 2026; Surana et al., 2023). This distinction is important because a mine haul route consists of multiple interconnected segments, each of which may exhibit different geometric and surface characteristics. Evaluating only average route conditions may therefore obscure local bottlenecks that disproportionately affect haul-truck speed and total cycle time. Existing studies have examined road-surface properties, vehicle selection, and individual cycle-time parameters. However, the integration of these aspects remains limited. This study addresses this gap by combining a comprehensive geometric audit of 38 road segments, rolling-resistance coefficients derived from field measurements, and TALPAC-based cycle-time modeling. This integrated approach provides a detailed assessment of the relationships among haul-road geometry, rolling resistance, and haul-truck performance along the study route.

This problem is particularly relevant to the Sector 7 haul route at PT Asmin Bara Bronang. An initial operational evaluation indicated that overburden haulage had not achieved the expected production target. Furthermore, the route comprises 38 individual segments with different geometric and surface characteristics that require technical assessment. These conditions directly influence the operating performance of the Komatsu HD785-7 haul trucks used for overburden transportation (Huang et al., 2026; Lalezar et al., 2024; Zhou et al., 2026). Therefore, identifying segments that fail to meet technical requirements and quantifying the operational effects of improving them are necessary to establish a more evidence-based foundation for haul-road redesign.

Accordingly, the research gap addressed in this study concerns the need for an integrated evaluation linking segment-level haul-road geometry, rolling resistance, haul-truck cycle time, and productivity improvement within a single analytical framework. Rather than treating geometric compliance and equipment productivity as separate engineering issues, this study evaluates their operational relationship by comparing existing road conditions with an improved-geometry scenario. The approach combines direct field measurements of road width, grade, superelevation, crossfall, and surface condition with operational cycle-time observations and TALPAC-based simulation.

The novelty of this study lies in integrating a geometric audit of all 38 existing haul-road segments, segment-level rolling-resistance assessment, compliance evaluation based on Ministerial Decree No. 1827 K/30/MEM/2018, and TALPAC simulation of haul-truck performance following geometric improvements. The study specifically aims to identify deficient road segments, determine the geometric modifications required to meet the applicable technical criteria, and estimate the resulting reduction in cycle time and increase in the productivity of Komatsu HD785-7 haul trucks. By establishing a measurable relationship between haul-road engineering improvements and operational performance, this study is expected to provide an empirical basis for decision-making at PT Asmin Bara Bronang, as well as a practical analytical framework that may be adapted to other open-pit mining operations experiencing comparable haulage constraints.

METHOD

This study employed a quantitative descriptive-evaluative research design to assess mine haul road geometry and its relationship with haul truck operating efficiency (Fan, Mao, Zhen, et al., 2026; Verma et al., 2025; Wang, Du, et al., 2025). The study was conducted along the Sector 7 overburden haul route of PT Asmin Bara Bronang, which extends 3,038 m from the pit to the disposal area and is divided into 38 segments. Primary data were obtained through direct field measurements of straight and curved road widths, longitudinal grades, superelevation, crossfall, road surface depressions, and the cycle times of Komatsu HD785-7 haul trucks during loading, loaded travel, dumping, return travel, and waiting. Comparable approaches to mine road and operational measurements are documented in the cited open-pit mining literature (Fan, Mao, Bao, et al., 2026; Wang et al., 2025; Zhao et al., 2025). The quantitative descriptive phase involved field measurements of (a) longitudinal grades using a laser theodolite at 50 m intervals across the 38 road segments; (b) road surface conditions, including surface texture and rut depth, using standardized measurement protocols; (c) rolling resistance using wheel-load sensors installed on an instrumented haul truck; and (d) operational cycle times obtained from the fleet monitoring system, yielding 47 complete haulage cycles. The evaluative phase comprised (1) comparing the measured values with the applicable technical criteria in Appendix II of Ministerial Decree No. 1827 K/30/MEM/2018; (2) simulating the baseline operating scenario using TALPAC; and (3) simulating an improved road geometry scenario. The relationships between road geometry, rolling resistance, and haul truck performance were evaluated using regression analysis and simulation-based sensitivity analysis.

Field measurements were supplemented with secondary company data, including current topographic maps, aerial photographs, overburden material characteristics, Dynamic Cone Penetrometer (DCP) test results, the existing Unsurfaced Road Condition Index (URCI), administrative boundary maps, and daily heavy equipment productivity records (Reddy et al., 2024; Zheng et al., 2024). The analysis proceeded by calculating the existing geometric

parameters, rolling resistance, and haul truck productivity for each of the 38 road segments; comparing the results with the applicable technical criteria in Appendix II of Ministerial Decree No. 1827 K/30/MEM/2018; redesigning noncompliant segments; and simulating travel speeds and cycle times under the improved geometric conditions using TALPAC. This sequence enabled a direct comparison of existing and improved haulage performance within a consistent computational framework (Chen et al., 2026; Ruiz-Vélez et al., 2026; Wu et al., 2024).

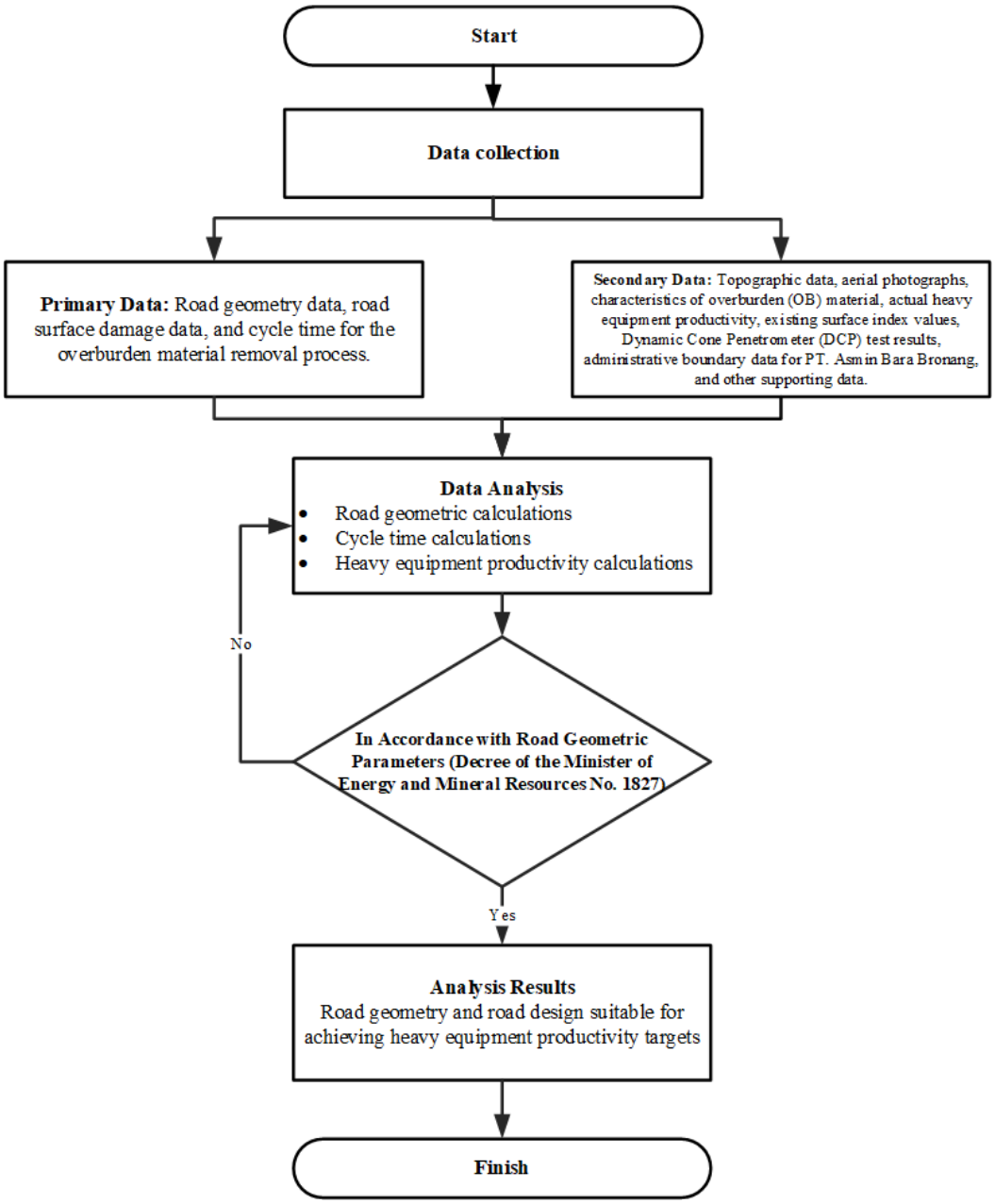


Figure 1. Research workflow

RESULTS AND DISCUSSION

Results

Actual Mine-Road Geometry

The overburden haul route from the mining front to the Sector 7 disposal area is 3,038 m long and is divided into 38 segments, comprising 26 straight segments and 12 curved segments. The following measurements characterize the existing road conditions.

Road Width

Road width was measured directly along each segment. The measured widths of the Sector

7 haul road are summarized in Table 1.

Table 1
Actual haul-road width

No.	Road Segment	Start STA (m)	End STA (m)	Length (m)	Width (m)	Condition
1	Segment 1	0	62	62	10.00	Straight
2	Segment 2	62	162	100	13.60	Straight
3	Segment 3	162	262	100	18.03	Straight
4	Segment 4	262	326	64	15.70	Straight
5	Segment 5	326	399	73	28.92	Curve
6	Segment 6	399	473	74	19.95	Straight
7	Segment 7	473	538	65	20.85	Curve
8	Segment 8	538	638	100	17.00	Straight
9	Segment 9	638	682	44	20.47	Straight
10	Segment 10	682	747	65	23.83	Curve
11	Segment 11	747	869	122	25.70	Straight
12	Segment 12	869	953	84	18.20	Curve
13	Segment 13	953	1053	100	21.43	Straight
14	Segment 14	1053	1171	118	21.09	Straight
15	Segment 15	1171	1244	73	24.00	Curve
16	Segment 16	1244	1333	89	21.96	Straight
17	Segment 17	1333	1406	73	20.45	Straight
18	Segment 18	1406	1506	100	19.53	Straight
19	Segment 19	1506	1561	55	21.27	Straight
20	Segment 20	1561	1623	62	19.60	Curve
21	Segment 21	1623	1723	100	25.20	Straight
22	Segment 22	1723	1771	48	24.15	Straight
23	Segment 23	1771	1867	96	24.85	Straight
24	Segment 24	1867	1967	100	24.06	Straight
25	Segment 25	1967	2014	47	30.81	Straight
26	Segment 26	2014	2076	62	29.72	Curve
27	Segment 27	2076	2155	79	23.52	Straight
28	Segment 28	2155	2239	84	20.93	Curve
29	Segment 29	2239	2309	70	22.64	Straight
30	Segment 30	2309	2379	70	24.00	Curve
31	Segment 31	2379	2477	98	21.30	Straight
32	Segment 32	2477	2535	58	19.18	Straight
33	Segment 33	2535	2649	114	21.88	Curve
34	Segment 34	2649	2706	57	18.53	Straight
35	Segment 35	2706	2787	81	23.26	Curve
36	Segment 36	2787	2887	100	19.58	Straight
37	Segment 37	2887	2973	86	19.50	Straight
38	Segment 38	2973	3038	65	20.76	Curve

Road Grade

The existing road grades were derived from geodetic GPS measurements of coordinates and elevations. Table 2 presents the measured elevation differences, slope distances, horizontal distances, and calculated road grades.

Table 2
Actual mine-road grade

No.	Road Segment	Elevation Difference (m)	Slope Distance (m)	Horizontal Distance (m)	Road Grade (%)
1	Segment 1	-6.55	62	61.65	-10.62%

No.	Road Segment	Elevation Difference (m)	Slope Distance (m)	Horizontal Distance (m)	Road Grade (%)
2	Segment 2	3.9	100	99.92	3.90%
3	Segment 3	9.2	100	99.58	9.24%
4	Segment 4	5.13	64	63.79	8.04%
5	Segment 5	5.22	73	72.81	7.17%
6	Segment 6	5.52	74	73.79	7.48%
7	Segment 7	4.54	65	64.84	7.00%
8	Segment 8	3.45	100	99.94	3.45%
9	Segment 9	2.88	44	43.91	6.56%
10	Segment 10	5.85	65	64.74	9.04%
11	Segment 11	3.75	122	121.94	3.08%
12	Segment 12	1.46	84	83.99	1.74%
13	Segment 13	-2.88	100	99.96	-2.88%
14	Segment 14	0.63	118	118.00	0.53%
15	Segment 16	0.94	73	72.99	1.29%
16	Segment 17	-0.24	89	89.00	-0.27%
17	Segment 18	0.6	73	73.00	0.82%
18	Segment 19	5.74	100	99.84	5.75%
19	Segment 20	5.29	55	54.75	9.66%
20	Segment 21	1.67	62	61.98	2.69%
21	Segment 22	2.79	100	99.96	2.79%
22	Segment 23	0.76	48	47.99	1.58%
23	Segment 24	-3	96	95.95	-3.13%
24	Segment 25	-2.88	100	99.96	-2.88%
25	Segment 26	-3.1	47	46.90	-6.61%
26	Segment 27	-0.63	62	62.00	-1.02%
27	Segment 28	-2.13	79	78.97	-2.70%
28	Segment 29	-2.37	84	83.97	-2.82%
29	Segment 30	-1.17	70	69.99	-1.67%
30	Segment 31	-1.82	70	69.98	-2.60%
31	Segment 32	-1.2	98	97.99	-1.22%
32	Segment 33	-3.24	58	57.91	-5.59%
33	Segment 34	-0.64	114	114.00	-0.56%
34	Segment 35	-1.98	57	56.97	-3.48%
35	Segment 36	-3.6	81	80.92	-4.45%
36	Segment 37	-2.78	100	99.96	-2.78%
37	Segment 38	-1.67	86	85.98	-1.94%
38	Segment 39	-2.68	74	73.95	-3.62%

Superelevation

Superelevation was calculated for the curved road segments using the elevation difference between the outer and inner edges of each curve. The results are presented in Table 3.

Table 3

Actual mine-road superelevation

No.	Road Segment	Outer Elevation (m asl)	Inner Elevation (m asl)	Elevation Difference (m)	Width (m)	Superelevation (%)
1	Segment 5	87.75	87.35	0.40	28.92	1.4%
2	Segment 7	98.47	97.50	0.47	20.85	4.7%
3	Segment 10	108.91	108.52	0.39	23.83	1.6%
4	Segment 12	116.44	116.20	0.24	18.20	1.3%
5	Segment 15	115.45	115.20	0.25	24.00	1.0%
6	Segment 20	128.59	128.11	0.48	19.60	2.4%

No.	Road Segment	Outer Elevation (m asl)	Inner Elevation (m asl)	Elevation Difference (m)	Width (m)	Superelevation (%)
7	Segment 26	123.44	123.10	0.34	29.72	1.1%
8	Segment 28	119.35	119.15	0.20	20.93	1.0%
9	Segment 30	116.49	116.10	0.39	24.00	1.6%
10	Segment 33	110.36	110.08	0.28	21.88	1.3%
11	Segment 35	107.70	107.45	0.25	23.26	1.1%
12	Segment 38	99.27	99.25	0.02	20.76	0.1%

Crossfall

Crossfall was measured using a geological compass at three aligned points along each straight segment. The resulting transverse slopes are presented in Table 4.

Table 4
Actual mine-road crossfall

No.	Road Segment	Length (m)	Width (m)	Crossfall (%)
1	Segment 1	62	10.00	0.0%
2	Segment 2	100	13.60	1.0%
3	Segment 3	100	18.03	1.0%
4	Segment 4	64	15.70	2.0%
5	Segment 6	74	19.95	2.0%
6	Segment 8	100	17.00	1.0%
7	Segment 9	44	20.47	1.5%
8	Segment 11	122	25.70	2.0%
9	Segment 13	100	21.43	1.0%
10	Segment 14	118	21.09	2.0%
11	Segment 16	89	21.96	1.5%
12	Segment 17	73	20.45	1.0%
13	Segment 18	100	19.53	1.0%
14	Segment 19	55	21.27	2.0%
15	Segment 21	100	25.20	1.0%
16	Segment 22	48	24.15	0.0%
17	Segment 23	96	24.85	0.0%
18	Segment 24	100	24.06	0.0%
19	Segment 25	47	30.81	0.0%
20	Segment 27	79	23.52	0.0%
21	Segment 29	70	22.64	1.0%
22	Segment 31	98	21.30	0.5%
23	Segment 32	58	19.18	2.0%
24	Segment 34	57	18.53	0.5%
25	Segment 36	100	19.58	0.0%
26	Segment 37	86	19.50	0.0%

Rolling Resistance

Rolling resistance is the resistance opposing wheel movement as a tire interacts with the road surface. Segment-level values calculated from the observed surface conditions are presented in Table 5.

Table 5
Actual mine-road rolling resistance

No.	Road Segment	Length (m)	Width (m)	Rolling Resistance (%)	Condition
1	Segment 1	62	10.00	12.25	Straight
2	Segment 2	100	13.60	8.17	Straight

No.	Road Segment	Length (m)	Width (m)	Rolling Resistance (%)	Condition
3	Segment 3	100	18.03	2.45	Straight
4	Segment 4	64	15.70	3.27	Straight
5	Segment 5	73	28.92	1.63	Curve
6	Segment 6	74	19.95	1.63	Straight
7	Segment 7	65	20.85	2.45	Curve
8	Segment 8	100	17.00	2.45	Straight
9	Segment 9	44	20.47	1.63	Straight
10	Segment 10	65	23.83	2.45	Curve
11	Segment 11	122	25.70	3.27	Straight
12	Segment 12	84	18.20	3.27	Curve
13	Segment 13	100	21.43	2.45	Straight
14	Segment 14	118	21.09	2.45	Straight
15	Segment 15	73	24.00	2.45	Curve
16	Segment 16	89	21.96	2.45	Straight
17	Segment 17	73	20.45	3.27	Straight
18	Segment 18	100	19.53	9.80	Straight
19	Segment 19	55	21.27	2.45	Straight
20	Segment 20	62	19.60	8.17	Curve
21	Segment 21	100	25.20	4.08	Straight
22	Segment 22	48	24.15	2.45	Straight
23	Segment 23	96	24.85	2.45	Straight
24	Segment 24	100	24.06	3.27	Straight
25	Segment 25	47	30.81	2.45	Straight
26	Segment 26	62	29.72	7.35	Curve
27	Segment 27	79	23.52	2.45	Straight
28	Segment 28	84	20.93	2.45	Curve
29	Segment 29	70	22.64	2.45	Straight
30	Segment 30	70	24.00	2.45	Curve
31	Segment 31	98	21.30	1.63	Straight
32	Segment 32	58	19.18	1.63	Straight
33	Segment 33	114	21.88	2.45	Curve
34	Segment 34	57	18.53	2.45	Straight
35	Segment 35	81	23.26	2.45	Curve
36	Segment 36	100	19.58	4.08	Straight
37	Segment 37	86	19.50	3.27	Straight
38	Segment 38	74	20.76	9.80	Curve

Improved Mine-Road Geometry

The measured geometry of the Sector 7 haul road was evaluated against the parameters specified in Appendix II of Ministerial Decree No. 1827 K/30/MEM/2018. Segments that did not meet the specified requirements were recalculated and redesigned to satisfy the applicable operational criteria.

Haul-Road Width

The minimum haul-road width was determined based on the largest vehicle operating in Sector 7, the Komatsu HD 785-7 dump truck, which has a vehicle width of 6.8 m. For a two-way straight haul road, the minimum width was calculated as follows:

$$L_{min} = n \times W_t + (n + 1)(0.5 \times W_t) \quad (1)$$

$$L_{min} = 2 \times 6.8 + (2 + 1)(0.5 \times 6.8)$$

$$L_{min} = 23.8 \text{ m}$$

where Lmin is the minimum haul-road width (m), n is the number of lanes, and Wt is the haul-truck width (m).

For a two-way curved haul road, the calculation used a wheel-track width of 4.17 m, a

front-axle-to-front-overhang distance of 2.15 m, and a rear-axle-to-rear-overhang distance of 3.19 m. The turning allowances were calculated as follows:

$Fa = Ad \times \sin \alpha = 2.15 \times \sin 41° = 1.41$ m .....(2)

$Fb = Ab \times \sin \alpha = 3.19 \times \sin 41° = 2.09$ m .....(3)

$C = Z = (U + Fa + Fb) / 2 = 3.84$ m .....(4)

$Wmin = 2(U + Fa + Fb + Z) + C = 26.85$ m .....(5)

where Wmin is the minimum haul-road width on a curve, U is wheel-track width, Fa and Fb are front and rear overhang allowances, Z is edge clearance, C is inter-vehicle clearance, and Ad and Ab are the front and rear axle-overhang distances. Based on Table 1, 20 straight segments and 10 curved segments were below the calculated minimum. The required average widening is therefore 4.56 m for deficient straight segments and 5.10 m for deficient curves.

Road Grade

Ministerial Decree No. 1827 K/30/MEM/2018 permits mine-road grades of up to 12%, whereas PT Asmin Bara Bronang applies a more conservative operating limit of 8% to support traction and braking performance (Ministry of Energy and Mineral Resources of the Republic of Indonesia, 2018). Road grade was calculated from the elevation difference and horizontal distance using the following equation:

$Grade\ (\%) = (\Delta h / \Delta x) \times 100\%$ .....(6)

$Grade\ (\%) = (6.55 / 61.65) \times 100\% = 10.62\%$

Segment 1 therefore has an absolute grade of 10.62%. Table 2 indicates that four segments exceed the company's 8% operating limit. These segments require cutting to reduce their grades by an average of approximately 1.5 percentage points and bring the haul road within the target operating range.

Superelevation

Superelevation provides a transverse slope on curved road segments to help counteract the lateral effects associated with vehicle movement through curves. The operating criterion adopted in this study is a minimum superelevation of 4% (Ministry of Energy and Mineral Resources of the Republic of Indonesia, 2018). Eleven curved segments were below this threshold, requiring an average increase in superelevation of 2.7 percentage points.

Crossfall

A mine-road crossfall of at least 2% is required to drain rainfall from the running surface toward the roadside drainage system (Ministry of Energy and Mineral Resources of the Republic of Indonesia, 2018). Table 4 shows that 20 straight segments did not meet the 2% target, indicating the need for surface scraping and reshaping to establish adequate transverse drainage.

Rolling Resistance

The rolling-resistance calculation used the fully loaded mass of the HD 785-7, reported as 172 metric tonnes (379,194.6 lb), six tires, a tire radius of 53.15 in, and the measured surface depression. For Segment 2, which had a measured depression of 3.94 in, the calculation is illustrated below:

$W = \text{total loaded weight} / \text{number of tires} = 379{,}194.6 / 6 = 63{,}199.11$ lb/tire .....(7)

$F = (W \times a) / r = (63{,}199.11 \times 3.94) / 53.15 = 4{,}681.42$ lb/tire .....(8)

$Wtotal = F \times \text{number of tires} = 4{,}681.42 \times 6 = 28{,}088.49$ lb .....(9)

$RR = Wtotal / \text{loaded mass} = 28{,}088.49 / 172 = 163.3$ lb/ton .....(10)

Using the conversion adopted in this study, the resulting rolling-resistance coefficient is (163.3/20=8.17%). PT Asmin Bara Bronang uses 2.45% as the target rolling-resistance value for a well-maintained road surface. Fourteen segments exceeded this target and therefore require surface rehabilitation, guided by the Unsurfaced Road Condition Index, to achieve the target value of 2.45%.

Existing Cycle Time

Overburden haulage in Sector 7 uses Komatsu HD 785-7 dump trucks. The existing cycle

time was determined through observations covering the period from the start of loading to loaded travel, dumping, empty-return travel, and waiting before the next loading event. The total cycle time is expressed as follows:

CT = T1 + T2 + T3 + T4 + T5 .....(11)

CT = 1.8 + 13.3 + 0.5 + 10.32 + 1.17 = 26.99 min

where T1 is loading time, T2 is loaded-haul time, T3 is dumping time, T4 is empty-return time, and T5 is waiting time. The existing Komatsu HD 785-7 cycle time on the Sector 7 route is therefore 26.99 minutes.

TALPAC Simulation of Cycle Time and Travel Speed

The ideal-geometry scenario was simulated using TALPAC to estimate travel speeds and cycle times for individual road segments. The simulation incorporated the overburden characteristics, the Volvo FM 450 haul-truck configuration, and segment-level road parameters, including road length, grade, curve radius, superelevation, rolling resistance, and design speed. The operational inputs comprised a payload capacity of 80 tonnes, a bucket capacity of 11.5 m^3, a fill factor of 95% based on field observations, a material bulk density of 2.1 t/m^3, and a swell factor of 1.25.

Vehicle performance was modeled using the Volvo FM 450 engine-power specifications, with traction coefficients of 0.55 for ballasted surfaces and 0.60 for compacted surfaces. Maximum travel speeds were specified according to road gradient: 48 km/h for gradients of 0–5°, 38 km/h for 5–10°, 28 km/h for 10–15°, and 18 km/h for 15–20°. These gradient ranges should be verified because the road grades elsewhere in the study are expressed as percentages rather than degrees.

The cycle-time calculation included a field-measured average loading time of 3.2 minutes, a dumping time of 1.8 minutes, a waiting and spotting time of 0.9 minutes, and a modeled empty-return travel time based on segment distance and gradient. Rolling-resistance values were assigned to individual road segments using field-derived values ranging from 0.45 to 0.75. The resulting simulation profile is presented in Figure 2.

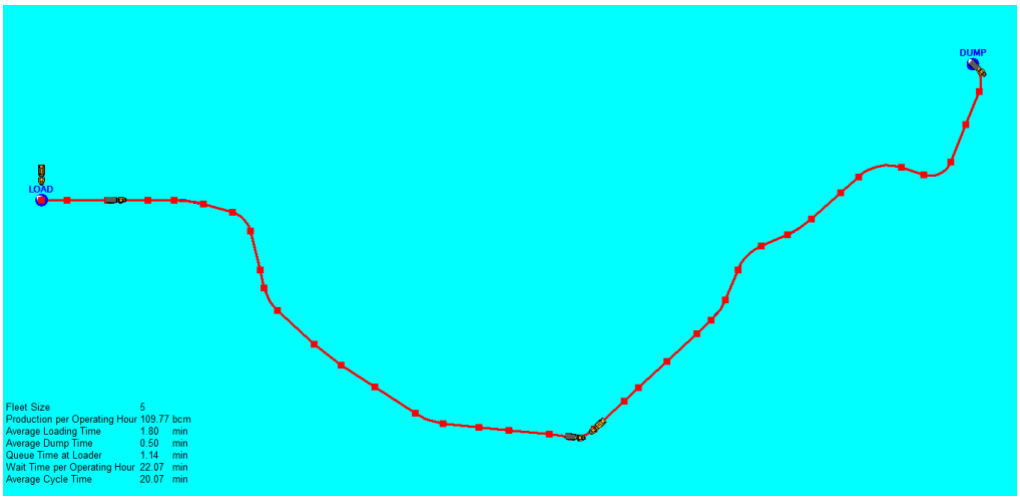


Figure 2. TALPAC simulation result

The TALPAC simulation produced a cycle time of 20.07 minutes and an average travel speed of 18.2 km/h under the ideal-geometry scenario. Relative to the existing cycle time of 26.99 minutes, the simulated cycle-time reduction is 6.92 minutes.

Komatsu HD 785-7 Productivity

Existing productivity is 92.627 bcm/hour. Under the ideal geometry, haul-truck productivity was calculated using the study equation:

Q = (n × Kb × 3600 × FF × Sf × Eff) / CT .....(12)

Q = 2500 / 20.07 = 124.564 bcm/hour

where Q is haul-truck production (m^3/hour), n is the number of bucket loads, Kb is bucket capacity (m^3), FF is bucket fill factor, Sf is swelling factor, Eff is haul-truck work efficiency, and CT

is cycle time (s). The ideal-geometry scenario therefore increases productivity from 92.627 to 124.564 bcm/hour, equivalent to a reported improvement of approximately 31.94 bcm/hour.

Discussion

The geometric assessment demonstrates that a substantial portion of the Sector 7 haul route does not satisfy the geometric and surface-condition criteria required for efficient two-way haulage. Twenty straight segments and ten curved segments were narrower than the calculated minimum widths, while four segments exceeded the company's 8% grade threshold. These deficiencies can create local bottlenecks, constrain vehicle maneuverability, and increase the traction and braking demands placed on fully loaded haul trucks. These findings are operationally relevant because haulage efficiency depends not only on equipment capacity but also on the physical conditions that govern attainable travel speeds and stable vehicle movement, consistent with the broader emphasis on productivity in mine-loading and hauling research (Basharaf et al., 2026).

The transverse-slope and surface-condition results reinforce this interpretation. Eleven curved segments had superelevation below 4%, and 20 straight segments had crossfall below 2%. Inadequate crossfall reduces the ability of the running surface to shed rainfall, allowing water to accelerate rutting and pothole formation. The resulting deterioration is reflected in the 14 segments whose rolling resistance exceeded the company's target of 2.45%, with measured values reaching 12.25%. In practical terms, road drainage, surface maintenance, and geometric correction are interdependent components of the haulage system rather than isolated design parameters.

Redesigning the road around the largest operating haul truck resulted in a minimum two-way width of 23.80 m for straight segments and 26.85 m for curved segments, together with targeted improvements in grade, superelevation, crossfall, and surface condition. When these changes were represented in TALPAC, the simulated cycle time decreased from 26.99 to 20.07 minutes, and productivity increased from 92.627 to 124.564 bcm/h, a gain of approximately 31.937 bcm/h, or 34.48%. These findings indicate that segment-level geometric optimization can translate road-condition improvements into measurable gains in simulated haulage performance.

Although the case study is site-specific, the combined workflow of geometric auditing, rolling-resistance assessment, and cycle-time simulation can be applied to other open-pit mining operations facing comparable haul-road constraints. This approach provides a practical link between local road engineering and broader concerns regarding mine-haulage efficiency. The improved-road scenario is projected to reduce haul-truck cycle time based on the TALPAC simulation. The estimated 34.48% productivity improvement represents a modeled outcome based on the proposed geometric improvements and the operational parameters specified in the simulation, rather than a gain confirmed through field measurements. Actual productivity improvements may vary because of differences between simulation assumptions and field conditions, including weather variability, equipment wear, and variations in material properties. Therefore, post-improvement field measurements are necessary to validate the predicted cycle-time reduction and determine the productivity gains achievable under actual operating conditions.

CONCLUSION

The evaluation of the 38-segment haul road in Sector 7 of PT Asmin Bara Bronang demonstrates that geometric optimization has substantial potential to improve haulage efficiency and productivity. The findings indicate that 20 straight segments require an average widening of 4.56 m, while 10 curved segments require an average widening of 5.10 m. Additional improvements include reducing the grades of four steep segments by an average of approximately 1.5 percentage points, increasing superelevation across 11 curves by an average of 2.7 percentage points, establishing a 2% crossfall on 20 straight segments, and rehabilitating the surfaces of 14 segments to achieve a rolling-resistance target of 2.45%.

Under the improved-geometry scenario, TALPAC simulation estimated a reduction in haul-truck cycle time from 26.99 to 20.07 minutes and an increase in productivity from 92.627 to 124.564 bcm/h, representing an improvement of approximately 31.937 bcm/h, or 34.48%. These

findings highlight the importance of integrating road-geometry assessment, rolling-resistance analysis, and cycle-time simulation to support evidence-based decisions in mine-haul-road management.

This study provides a practical framework for prioritizing geometric improvements to enhance operational performance in open-pit mining. However, the estimated productivity improvement is based on TALPAC simulation rather than post-implementation field measurements and should therefore be interpreted as a projected outcome. Actual performance may vary depending on the quality of road improvements, equipment condition, operational consistency, material characteristics, and weather conditions. Accordingly, future research should validate the simulation results through field monitoring following road rehabilitation and examine the long-term implications for fuel consumption, road-maintenance costs, equipment performance, and haul-truck operational safety. Such validation would strengthen the applicability of the proposed optimization framework and support more reliable and sustainable haulage operations.

ACKNOWLEDGEMENT

The authors would like to express their sincere gratitude to PT Asmin Bara Bronang, particularly the management and technical teams involved in the Sector 7 mining operation, for providing valuable support, field access, operational data, and assistance during the data collection process. The authors also acknowledge all personnel who contributed to the measurement of haul-road geometry, rolling resistance assessment, and haul-truck cycle-time observations required for this research. The authors further express their appreciation to the Faculty of Engineering, Universitas Krisnadwipayana, for the academic support and facilities provided throughout this study. The authors gratefully acknowledge all individuals and organizations who directly or indirectly contributed to the successful completion of this research.

AUTHOR CONTRIBUTION STATEMENT

Achmad Pahrul Rodji contributed to the conceptualization of the research, methodology development, field data collection, analysis of mine haul-road geometry, evaluation of rolling resistance, haul-truck cycle-time assessment, data interpretation, and preparation of the manuscript. Indriasari contributed to the research methodology, validation of the analysis approach, interpretation of the findings, academic supervision, and refinement of the research framework. Rifki Hilmansyah contributed to data processing, simulation analysis using TALPAC, evaluation of haul-truck productivity, visualization of research results, and manuscript improvement. All authors contributed to the discussion and interpretation of the research findings and approved the final version of the manuscript. They also agreed to be accountable for all aspects of the work.

REFERENCES

Alshboul, O., Al-Shboul, K., Shehadeh, A., & Tatari, O. (2026). Advancing equipment management for construction: Introducing a new model for cost, time and quality optimization. *Construction Innovation*, *26*(4), 1191–1217. https://doi.org/10.1108/CI-04-2024-0129

Ascaso Til, M., & Wong, W. (2023). Examples of integrating hydraulic equipment into temporary works. *Proceedings of the Institution of Civil Engineers - Civil Engineering*, *176*(5), 28–39. https://doi.org/10.1680/jcien.22.00150

Basharaf, M., Sayadi, A. R., & Rahimdel, M. J. (2026). Improving productivity in mine loading and hauling operations through OEE analysis. *Resources Policy*, *115*, 105873. https://doi.org/10.1016/j.resourpol.2026.105873

Chen, Z., et al. (2026). Multi-modal vehicle trajectory prediction via hierarchical attention and raster-vector maps encoding in unstructured road environments. *Engineering Applications of Artificial Intelligence*, *167*, 113819. https://doi.org/10.1016/j.engappai.2026.113819

Fan, S., Mao, Y., Bao, N., He, L., Wen, J., & Mao, X. (2026). RoadMamba-Net: Intelligent road extraction from high-resolution optical satellite imagery for open-pit mining. *Optics & Laser Technology*, *204*, 116179. https://doi.org/10.1016/j.optlastec.2026.116179

Fan, S., Mao, Y., Zhen, S., Liu, J., He, L., & Mao, X. (2026). A novel framework for segmenting open-pit

mining road. *Engineering Applications of Artificial Intelligence*, *163*, 112811. https://doi.org/10.1016/j.engappai.2025.112811

Feng, J., Chen, W., Liu, C., Liu, X., Cao, B., & Xu, F. (2025). Advancements and challenges in earthmoving equipment automation using core technologies. *Automation in Construction*, *179*, 106472. https://doi.org/10.1016/j.autcon.2025.106472

Görçün, Ö. F., Chatterjee, P., Stević, Ž., & Küçükönder, H. (2024). An integrated model for road freight transport firm selection in third-party logistics using T-spherical fuzzy sets. *Transportation Research Part E: Logistics and Transportation Review*, *186*, 103542. https://doi.org/10.1016/j.tre.2024.103542

Huang, Y., Guo, Y., Zhang, S., Lu, L., Ai, Y., & Ge, S. (2026). Knowledge-driven MOEA/D for optimizing the road network of open-pit mines. *Expert Systems with Applications*, *326*, 132562. https://doi.org/10.1016/j.eswa.2026.132562

Jafarsalehi, M., Mashayekh, M., Miranzadeh, M. B., Mirzaei, N., & Ebrahimi, M. (2025). Primary measures for cleaner biomass combustion to reduce NOx: A narrative review on solid biomass fuels, NOx sources, small-scale boilers, axillary equipment, fuel management and fuel quality improvement. *Fuel*, *396*, 134891. https://doi.org/10.1016/j.fuel.2025.134891

Jerden, J., Mejbel, M., Filho, A. N. Z., Carroll, M., & Campe, J. (2024). The impact of geochemical and life-cycle variables on carbon dioxide removal by enhanced rock weathering: Development and application of the Stella ERW model. *Applied Geochemistry*, *167*, 106002. https://doi.org/10.1016/j.apgeochem.2024.106002

Kodikara, J., Sounthararajah, A., & Chen, L. (2024). Reimagining unbound road pavement technology: Integrating testing, design, construction and performance in the post-digital era. *Transportation Geotechnics*, *47*, 101274. https://doi.org/10.1016/j.trgeo.2024.101274

Lalezar, M., Izadi, I., Hoseinie, S. H., & Mohamadrezaie, H. (2024). A model predictive control algorithm for autonomous mining dump trucks. *IFAC-PapersOnLine*, *58*(22), 60–65. https://doi.org/10.1016/j.ifacol.2024.09.291

Ministry of Energy and Mineral Resources of the Republic of Indonesia. (2018). *Keputusan Menteri Energi dan Sumber Daya Mineral Republik Indonesia Nomor 1827 K/30/MEM/2018 tentang pedoman pelaksanaan kaidah teknik pertambangan yang baik* [Decree No. 1827 K/30/MEM/2018 on guidelines for implementing good mining engineering practices].

Mousavi, M., Shen, X., Zhang, Z., Barati, K., & Li, B. (2025). IoT-Bayes fusion: Advancing real-time environmental safety risk monitoring in underground mining and construction. *Reliability Engineering & System Safety*, *256*, 110760. https://doi.org/10.1016/j.ress.2024.110760

Reddy, A. S., Patil, M., Dalal, P. H., Iyer, K. K. R., & Dave, T. N. (2024). Sustainable utilization of landfill mined soil like fraction in subbase layer for asphalt road applications. *Cleaner Materials*, *11*, 100218. https://doi.org/10.1016/j.clema.2024.100218

Ruiz-Vélez, A., Sánchez-Garrido, A. J., Alcalá, J., & Yepes, V. (2026). Life-cycle environmental and social trade-offs in concrete road frame systems. *Cleaner Environmental Systems*, *22*, Article 100462. https://doi.org/10.1016/j.cesys.2026.100462

Saputra, Z., Sakti, A. D., Firmana, A., Ignatius, M., Hede, A. N. H., & Saepuloh, A. (2023). Enhanced mine road monitoring using unmanned aerial vehicles and deep-learning approach. *Remote Sensing Applications: Society and Environment*, *32*, 101080. https://doi.org/10.1016/j.rsase.2023.101080

Soto-Diaz, J., et al. (2026). The economics of mine waste reduction: The case of ore-sand. *Journal of Cleaner Production*, *573*, Article 148930. https://doi.org/10.1016/j.jclepro.2026.148930

Surana, V., Celentano, J., Raju, G. V. R., & Swami, M. M. (2023). Overcoming tunnelling challenges on the Mumbai Coastal Road project in India. *Proceedings of the Institution of Civil Engineers - Civil Engineering*, *176*(3), 113–120. https://doi.org/10.1680/jcien.22.00213

Verma, G. P., et al. (2025). Radiological considerations in using uranium mine waste rock for road construction materials. *Journal of Environmental Radioactivity*, *282*, 107613. https://doi.org/10.1016/j.jenvrad.2024.107613

Wang, J., Du, C., Luo, Z., & Ding, X. (2025). Study on starting mechanism and chemical control of road dust under disturbance of automobile tire in open-pit mine. *Journal of Environmental Chemical Engineering*, *13*(3), 116631. https://doi.org/10.1016/j.jece.2025.116631

Wang, J., et al. (2025). Experimental and numerical simulation of road dust distribution and transport characteristics under disturbance of automobile tire in open-pit mine. *Journal of Wind Engineering and Industrial Aerodynamics*, *266*, 106214. https://doi.org/10.1016/j.jweia.2025.106214

Wu, X., et al. (2024). Highly radiogenic lead in Shandong bronzes (5th–3rd century BC) and lead mines provides evidence of a metal road from China to Korea and Japan. *Journal of Archaeological Science*, *170*, 106047. https://doi.org/10.1016/j.jas.2024.106047

Yang, X., Zhang, J., Liu, W., Jing, J., Zheng, H., & Xu, W. (2024). Automation in road distress detection, diagnosis and treatment. *Journal of Road Engineering*, *4*(1), 1–26. https://doi.org/10.1016/j.jreng.2024.01.005

Yang, Y., Zhou, W., Jiskani, I. M., & Wang, Z. (2024). Extracting unstructured roads for smart open-pit mines based on computer vision: Implications for intelligent mining. *Expert Systems with Applications*, *249*, 123628. https://doi.org/10.1016/j.eswa.2024.123628

Zhao, H., Zheng, W., Qin, B., Ding, Z., Zhao, G., & Guo, P. (2025). Research on evolution model of road network for self-driving truck in open-pit mine. *Computers & Industrial Engineering*, *205*, 111166. https://doi.org/10.1016/j.cie.2025.111166

Zheng, C., Liu, L., Meng, Y., Wang, M., & Jiang, X. (2024). Passable area segmentation for open-pit mine road from vehicle perspective. *Engineering Applications of Artificial Intelligence*, *129*, Article 107610. https://doi.org/10.1016/j.engappai.2023.107610

Zhou, J., Xi, Y., Qin, H., Wang, C., & Zheng, N. (2026). Policy sandboxes for autonomous transportation in controlled environments: Evidence and insights from open-pit mining operations. *Transport Policy*, *185*, Article 104218. https://doi.org/10.1016/j.tranpol.2026.104218